ChemComm

Selective catalytic 2e⁻-oxidation of organic substrates by an Fe^{II} complex having an *N*-heterocyclic carbene ligand in water

Journal:	*ChemComm*
Manuscript ID	CC-COM-05-2020-003289.R1
Article Type:	Communication

COMMUNICATION

Selective catalytic 2e⁻-oxidation of organic substrates by an Fe^{II} complex having an *N*-heterocyclic carbene ligand in water

Received 00th January 20xx,
Accepted 00th January 20xx

DOI: 10.1039/x0xx00000x

Hiroto Fujisaki,[a] Tomoya Ishizuka,[a] Yoshihiro Shimoyama,‡[a] Hiroaki Kotani,[a] Yoshihito Shiota,[b,c] Kazunari Yoshizawa[b,c] and Takahiko Kojima*[a,c]

An Fe^{II} complex, 1, having a pentadentate ligand with an NHC moiety catalyzes substrate oxidation to afford 2e⁻-oxidized products with high selectivity by suppression of overoxidation in water. A Bell-Evance-Polanyi plot for the substrate oxidation catalyzed by 1 exhibited an inflection point around 86 kcal mol^{-1}, indicating strong C-H abstraction ability of the reactive species derived from 1.

High-valent Fe-oxo complexes have been well explored as important reactive species in oxidation reactions performed by metalloenzymes and synthetic oxidation reactions.[1–3] For example, nonheme iron enzymes such as α-ketoglutarate-dependent taurine dioxygenase (TauD)[4] generate an Fe^{IV}-oxo intermediate as the reactive species to hydroxylate taurine. The activation of C-H bonds by the Fe^{IV}-oxo species is proposed to occur through hydrogen-atom abstraction mechanism.[5,6] Oxidation enzymes such as TauD are able to oxidize substrates selectively to the corresponding 2e⁻-oxidized products.[4] A lot of synthetic Fe^{IV}-oxo complexes have been prepared and characterised to explore the reactivity of those complexes and to gain mechanistic insights into C-H oxidation.[7–9] However, these synthetic nonheme Fe^{IV}-oxo complexes do not perform selective 2e⁻ oxidation in organic solvents and aqueous media.[9] For example, an Fe^{IV}-oxo complex has been reported to oxidize ethylbenzene, toluene and cyclohexane to 1-phenylethanol (58% yield), benzaldehyde (58%) and cyclohexanone (57%), respectively, in CH_3CN.[9] Therefore, catalysts that can oxidize substrates to selectively afford 2e⁻-oxidation products in aqueous media are required to establish a sustainable oxidation strategy.

In general, a relationship between the activation energies for substrate oxidation and bond dissociation energies (BDEs) of the substrates can be analysed in light of the Bell-Evans-Polanyi (BEP) equation[10] as given bellow:

$$E_a = \alpha\Delta H + C \quad (1)$$

In most cases, oxidation reactions of C-H bonds by metal-oxo complexes obeyed the BEP relation.[11,12] However, the improvement of product selectivity in substrate oxidation have never been examined on the basis of the difference in BDEs between substrates and the corresponding oxidation products.

On the other hand, Long and co-workers have reported selective 2e⁻-oxidation by low-spin Fe^{IV}-oxo complexes with a pentadentate pyridyl ligands in aqueous media.[13] Furthermore, they also have reported that an Fe^{II}-acetonitrile complex having a pentadentate ligand with an *N*-heterocyclic carbene (NHC) moiety at the axial position.[14] In this case, the NHC moiety of the ligand exerts strong σ-donation and *trans*-influence as represented by a longer coordination bond between the Fe^{II} centre and the CH_3CN ligand.[14] Influence of an NHC ligand located at the *trans* position to an oxo ligand on the reactivity should be of interest in terms of the regulation of the reactivity of a high-valent Ru-oxo complex.[15–17] For such a Fe^{II}-NHC complex,[14] however, the reactivity in substrate oxidation has yet to be explored.

Herein, we report a novel Fe^{II}-aqua complex having a pentadentate ligand with an NHC moiety, $[Fe(PY_4Cl_2BIm)(OH_2)](NO_3)_2$ (**1**·$(NO_3)_2$) (PY_4Cl_2BIm: 5,6-dichloro-1,3-dihydro-1,3-bis(2-pyridyl)-methyl-2*H*-benz-imidazol-2-ylidene) as an efficient catalyst for substrate oxidation in water. In this study, we have focused on the catalytic oxidation by using complex **1**·$(NO_3)_2$ as a catalyst, $Na_2S_2O_8$ as a sacrificial electron-transfer (ET) oxidant in water to observe selective 2e⁻-oxidation of substrates. Synthesis of **1**·$(NO_3)_2$ was performed as described in Scheme 1 and the details are given in the ESI†. Characterization of the low-spin Fe^{II} complex was made by ^1H NMR (Fig. S1) and UV-vis absorption

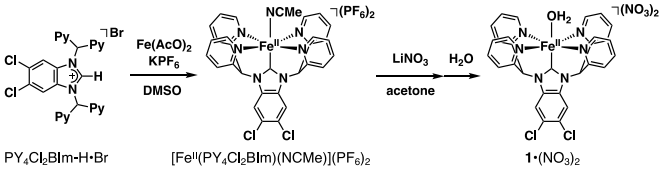

[a] *Department of Chemistry, Faculty of Pure and Applied Sciences, University of Tsukuba, 1-1-1 Tennoudai, Tsukuba, Ibaraki 305-8571, Japan*
[b] *Institute for Materials Chemistry and Engineering, Kyushu University, Moto-oka, Nishi-Ku, Fukuoka 819-0395, Japan*
[c] *CREST, Japan Science and Technology Agency (JST), Japan*
‡ *Present address: Interdisciplinary Research Centre for Catalytic Chemistry, National Institute of Advanced Industrial Science and Technology (AIST), 1-1-1 Higashi, Tsukuba, Ibaraki 305-8565, Japan*
† Electronic Supplementary Information (ESI) available: Further experimental details, supporting figures and tables. See DOI: 10.1039/x0xx00000x

Scheme 1. Synthesis of an Fe^{II}(NHC)-aqua complex, **1**·$(NO_3)_2$.

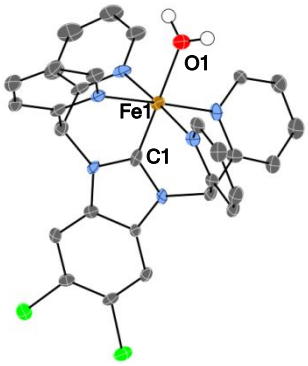

Fig. 1 An ORTEP drawing of the cation moiety of **1**·$(ClO_4)_2$ with 50% probability thermal ellipsoids. Hydrogen atoms except for the aqua ligand and two ClO_4^- ions are omitted for clarity. Grey, carbon; blue, nitrogen; red, oxygen; light green, chlorine.

spectroscopies, ESI-TOF-MS spectrometry (Fig. S2), X-ray crystallography, and elemental analysis. The crystal structure of **1**·$(ClO_4)_2$ (for preparation, see ESI) in place of **1**·$(NO_3)_2$ indicates that the NHC moiety of the PY_4Cl_2BIm ligand binds at the *trans*-position of the aqua-ligand as shown in Fig. 1. The Fe-O bond length of **1**·$(ClO_4)_2$ is 2.012(5) Å[18] and longer than that of the pyridyl counterpart (1.9907(13) Å),[13] indicating that the NHC ligand exerts strong *trans*-influence.

Electrochemical studies of **1**·$(NO_3)_2$ were performed in water in the presence of 0.1 M KNO_3 as an electrolyte to observe a reversible redox wave of **1**·$(NO_3)_2$ at +0.38 V (*vs.* SCE), indicating that the Fe^{II} centre was oxidized to the Fe^{III} state (Fig. S3). The Fe^{III} centre was confirmed to be in a low-spin (S = 1/2) state by ESR spectroscopy at 5 K after a reaction of **1**·$(NO_3)_2$ with $(NH_4)_2$-$[Ce^{IV}(NO_3)_6]$ (CAN) in water (Fig. S4). In the Pourbaix diagram of **1**, the Fe^{II}/Fe^{III} redox potential of **1** in water showed no dependence on solution pH values (Fig. S5). Since the acidity of the aqua ligand in **1**·$(NO_3)_2$ decreased due to the strong *trans*-influence of the NHC ligand, the pK_a value of the aqua ligand could not be determined in the pH range from 1.0 to 12 by UV-vis spectroscopic titration (Fig. S6). Thus, $1e^-$ oxidation of **1**·$(NO_3)_2$ forms the corresponding Fe^{III}-OH_2 complex in the pH range. Note that, in CH_2Cl_2, two oxidation waves were observed in a square-wave voltammogram; the first one at +0.60 V (*vs.* SCE) should be due to the Fe^{II}/Fe^{III} process and the second one at +1.92 V should be due to oxidation of the Fe^{III} complex to an Fe^{IV} species (Fig. S7).

Catalytic oxidation was performed in a glass tube containing D_2O (1.0 mL, pD was not adjusted), **1**·$(NO_3)_2$ (0.1 mM), oxidant (50 mM) and a substrate (10 mM) at 323 K under Ar atmosphere. Catalytic turnover numbers (TONs) after stirring for 3 h were determined by ^{1}H NMR spectroscopy using sodium trimethylsilylpropanesulfonate (DSS) as an internal standard. Here, sodium ethylbenzenesulfonate (EtPhS), sodium cumenesulfonate (CumS) and sodium styrenesulfonate (StyS) were used as water-soluble substrates. At first, we explored the reactivity of various oxidants in the presence of **1**·$(NO_3)_2$ and consequently $Na_2S_2O_8$ was found to be the best oxidant among them (Table S1). In addition, the ESI-TOF-MS measurement of the mixture after the catalytic reaction indicates that the Fe^{III} species remaining in the solution is an $Fe(PY_4Cl_2BIm)$ complex having the substrate as a ligand (Fig. S8). Thus, complex **1** still holds the PY_4Cl_2BIm ligand even after the reaction. The TONs obtained for three substrates with $Na_2S_2O_8$ are listed in Table 1. Formation of CO_2 and O_2 was not observed in GC-MS measurements for the reaction mixtures in all cases. In the case of oxidation of EtPhS and CumS, the $2e^-$ oxidation proceeded to afford the corresponding benzyl alcohol derivatives in TONs of 42 and 26, respectively.[19] In the EtPhS oxidation, $CH_3CH(OH)PhS$ was obtained in 86% selectivity; however, catalytic oxidation of EtPh by a nonheme Fe^{IV}-oxo complex has been reported to afford $CH_3CH(OH)Ph$ in *ca.* 50% selectivity.[9,20] Oxidation of StyS selectively afforded a diol derivative, which should be derived from hydrolysis of the corresponding epoxide as a $2e^-$-oxidized product, in full conversion. On the other hand, $2e^-$-oxidation products were not observed in the absence of catalyst **1**·$(NO_3)_2$ (Table S2). These results indicate that **1**·$(NO_3)_2$ selectively catalyses $2e^-$-oxidation of substrates by suppression of over-oxidation.

Table 1 Catalytic substrate oxidation by **1**·$(NO_3)_2$ in water

Substrate	Product	TONs[a]	Alcohol/ketone	Conversion, %
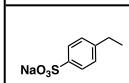 EtPhS	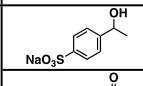	42	6.0	49
	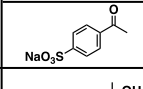	7		
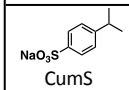 CumS	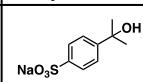	26	–	26
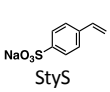 StyS	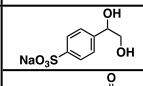	93	23	97
	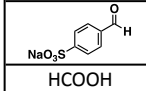	2		
	HCOOH	2		

[a] TONs = [Product]/[catalyst]. Conditions: [**1**·$(NO_3)_2$] = 0.1 mM, [$Na_2S_2O_8$] = 50 mM, [Substrate] = 10 mM, T = 323 K, and reaction time = 3 h. TONs were determined by ^{1}H NMR spectroscopy using DSS as an internal standard. Any side-reaction products except those listed in the table were not observed.

To confirm the origin of the oxygen atoms of $CH_3CH(OH)PhS$ obtained from the oxidation reaction of EtPhS, ^{18}O-labeled water ($H_2{}^{18}O$) was used as a solvent. In the ESI-TOF-MS spectrum of the reaction mixture in $H_2{}^{18}O$, a peak cluster was observed at m/z = 203.17 for $CH_3CH(^{18}OH)PhS$, not at m/z = 201.10 for $CH_3CH(^{16}OH)PhS$ (Fig. S9). This indicates that $Na_2S_2O_8$ works simply as an ET oxidant, not as an oxygen-atom-transfer reagent in the reaction.[21] Thus, it has been confirmed that an oxygen atom in the active species derived from water as a solvent is transferred to a substrate, affording an oxygenated product.

To gain mechanistic insights into the oxidation process of EtPhS, kinetic studies were performed. At first, catalytic oxidation reactions of EtPhS were conducted in D_2O (pD was not adjusted) in the presence of $Na_2S_2O_8$ (50 mM) and various concentration of **1**·$(NO_3)_2$ (0.01–0.1 mM) at 323 K and the progress of the reaction was monitored by ^{1}H NMR spectroscopy. The initial rates, v_0, were determined with the

slope of time-course of the $CH_3CH(OH)PhS$ formation (Fig. S11). On the basis of the dependence of v_0 on the concentration of **1**·$(NO_3)_2$ obeyed first-order kinetics (Fig. 2a). Thus, one molecule of the catalyst participates in the catalytic oxidation of EtPhS. Based on this dependence, the rate constants, k_{cat}, were determined. The k_{cat} values were also determined for various initial concentrations of EtPhS (Fig. 2b). As the results, saturation of k_{cat} values against the concentration of EtPhS was observed, indicating that the existence of a pre-equilibrium process between an oxidatively active species and EtPhS prior to the oxidation. Curve fitting for the plots of k_{cat} against the concentration of EtPhS with eq (2)[22,23] afforded the equilibrium constant, K, as (1.3 ± 0.2) × 10^2 M^{-1} for the pre-equilibrium process and the first-order rate constant, k, as (7.9 ± 0.4) × 10^{-3} s^{-1} for the oxidation reaction (Table S3).

$$k_{cat} = kK[EtPhS]/(1 + K[EtPhS]) \quad (2)$$

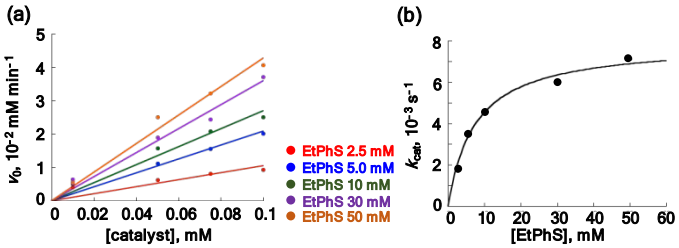

Fig. 2 (a) Dependence of the initial rates on the catalyst concentration, and (b) dependence of the rate constants, k_{cat}, on the initial concentration of EtPhS for the oxidation of EtPhS by **1**·$(NO_3)_2$ as the catalyst (0.1 mM) and $Na_2S_2O_8$ as an oxidant (50 mM) in D_2O (pD was not adjusted) at 323 K.

To obtain further information on the oxidation process by **1**·$(NO_3)_2$, the kinetic isotope effects (KIE) were also studied using sodium triphenylmethanesulfonate (TPMS) and its mono-deuterated derivative (TPMS-d_1) in a D_2O solution at 323 K and the reactions were monitored by ^1H NMR spectroscopy. The k_{cat} values for the TPMS and TPMS-d_1 oxidation also displayed saturation behaviour as in the case of EtPhS oxidation described above (Fig. 3). The k and K values were also determined for TPMS (k^H = (4.4 ± 0.1) × 10^{-3} s^{-1}, K^H = (1.9 ± 0.3) × 10^2 M^{-1}) and TPMS-d_1 (k^D = (1.2 ± 0.5) × 10^{-3} s^{-1}, K^D = 46 ± 5 M^{-1}) based on eq 2 (Table S3). The oxidation of TPMS-d_1 was clearly slower than that of TPMS. The KIE value was determined to be 3.7 as the ratio of the rate constants (k^H/k^D) for the oxidation reactions of TPMS and TPMS-d_1. The KIE value indicates that the hydrogen-atom abstraction from the methine C-H bond is involved in the rate-determining step (RDS).

To investigate the dependence of the k values on BDEs of the C-H bonds for substrates, we determined the k values for oxidation of six substrates, TPMS (BDE = 79.0 kcal mol^{-1}),[24] sodium diphenylmethane-sulfonate (DPMS; 82.0),[24] CumS (83.5),[24] EtPhS (85.4),[24] benzyl alcohol (BnOH; 87.5),[24] 2-propanol (2-PrOH; 90.0),[24] by **1**·$(NO_3)_2$ as the catalyst and $Na_2S_2O_8$ as the sacrificial oxidant at 323 K (Table S3). The log (k/n) values (n: the number of equivalent C-H hydrogen atoms) were plotted against the BDE values of the C-H bonds to be cleaved in the substrates (Fig. 4). In contrast to other Fe catalysts,[11,12] the rate constants for the oxidation reactions by **1**·$(NO_3)_2$ showed an inflection point: For substrates having BDE values greater than *ca.* 86 kcal mol^{-1}, the log (k/n) values decreases with increasing BDE as expected on the basis of the eq (1) with α = –0.5. In sharp contrast, for substrates having BDEs less than *ca.* 86 kcal mol^{-1}, log (k/n) values showed no dependence on the BDE values.

Tanko and co-workers have reported on oxidation reactions of organic substrates by $^tBuO^•$ as the oxidant and discussed causes of the insensitivity of the rate constants to the BDEs of the C-H bonds in substrates.[25] It has been known that the BDE of the O-H bond in ^{t}BuOH is 105 kcal mol^{-1}, indicating that $^tBuO^•$ has high reactivity in hydrogen-atom abstraction. Furthermore, their BEP plot for oxidation of various substrates by $^tBuO^•$ exhibited an inflection point at *ca.* 92 kcal mol^{-1}, which is about 13 kcal mol^{-1} lower than that of the O-H bond of ^{t}BuOH. Therefore, our results suggest that the O-H bond formed after C-H oxidation in a putative Fe-oxo reactive species derived from **1**·$(NO_3)_2$ should have a large BDE value (*ca.* 100 kcal mol^{-1}), in light of the inflection point at *ca.* 86 kcal mol^{-1}.

The relatively high 2e$^-$-oxidation selectivity by suppression of overoxidation in the present system should be derived from a strongly BDE-controlled reaction mechanism as demonstrated by the BEP plot (Fig. 4): C-H abstraction from the 1-phenyl-ethanol derivative (BDE: 88.3 kcal mol^{-1})[24] as the 2e$^-$-oxidized product of EtPhS (85.4 kcal mol^{-1}) should be strongly retarded, in light of the BEP plot. On the basis of the product analysis and kinetic studies described above, a plausible mechanism for the oxidation reaction of EtPhS catalysed by **1**·$(NO_3)_2$ is proposed as shown in Fig. 5. As the first step, **1** is oxidized to the corres-

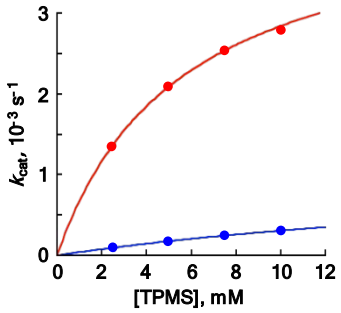

Fig. 3 Pseudo-first-order kinetic analysis for oxidation reactions of TPMS (red line) and TPMS-d_1 (blue line) by **1**·$(NO_3)_2$ as the catalyst (0.1 mM) and $Na_2S_2O_8$ as oxidant (50 mM) in D_2O (pD was not adjusted) at 323 K.

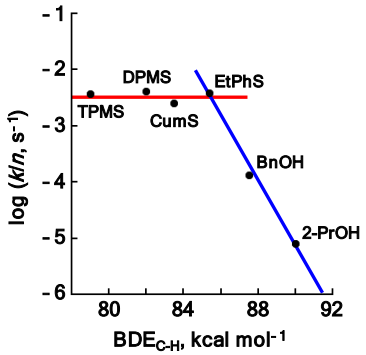

Fig. 4 A plot of the log (k/n) at 323 K for the oxidation of five substrates (TPMS, DPMS, CumS, EtPhS, BnOH, and 2-PrOH) by **1** against BDEs of C-H bonds to be cleaved.

ponding Fe^{III}-OH_2 complex through ET oxidation by $S_2O_8^{2-}$, as confirmed by ESR spectroscopy after the reaction of **1**·$(NO_3)_2$ with $Na_2S_2O_8$ (step I in Fig. 5; see Fig. S12). The Fe^{III}-OH_2 complex is further oxidized by $SO_4^{\bullet-}$ to form an Fe^{IV}=O active species, which is known to exhibit extremely strong oxidizing power,[26] enough to oxidize the Fe^{III}-OH_2 complex to the Fe^{IV}=O complex; $E(Fe^{III}/Fe^{IV})$ = +1.92 V *vs.* SCE in CH_2Cl_2 (see above, step II). To clarify the characteristics of the reactive species formed by 2e⁻-oxidation of **1**, DFT calculations were performed on a Fe-O complex including two H_2O molecules interacted with the oxygen ligand at the B3LYP/6-311+G** level of theory (Fig. S13). The results suggest that the triplet Fe^{IV}=O state is the most stable (Table S4). The Fe=O distance in the optimized structure is 1.668 Å and the bond order is 1.83. After the pre-equilibrium process to form an adduct between the active species and EtPhS (step III, see Fig. 2), EtPhS is oxidized through the C-H bond cleavage as the RDS to afford the 2e⁻-oxidized product (step IV, KIE shown in Fig. 3). In the final step V, the oxidized product coordinated to Fe centre is substituted by a water molecule to complete the catalytic cycle (see Fig. S9).

In conclusion, we have demonstrated catalytic oxidation reactions by an NHC-ligated Fe-complex, **1**·$(NO_3)_2$ as a catalyst to afford 2e⁻-oxidized products with high selectivity by suppression of overoxidation in water. Although details of the reactive species in the reactions have yet to be clarified, the reactive species derived from **1** should have a strong oxidative activity due to the strong *trans*-influence from the NHC moiety.

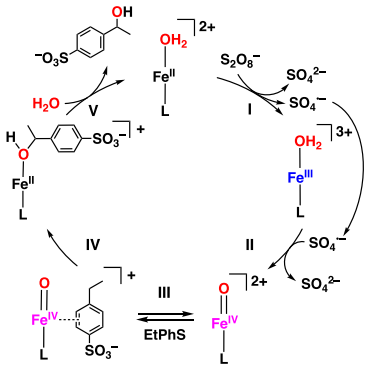

Fig. 5 A proposed mechanism of the oxidation of EtPhS by **1** and $S_2O_8^{2-}$.

This work has been supported by JST CREST (Grant JPMJCR16P1) and Grants-in-Aid (15H00915, 17H03027, and 18K19089) from the Japan Society of Promotion of Science (JSPS).

Conflicts of interest

There are no conflicts to declare.

Notes and references

1 M. Costas, M. P. Mehn, M. P. Jensen and L. Que Jr., *Chem. Rev.,* 2004, **104**, 939-986.
2 M. Ekroos and T. Sjogren, *Proc. Natl. Acad. Sci. U. S. A.,* 2006, **103**, 13682-13687.
3 I. G. Denisov, T. M. Makris, S. G. Sligar and I. Schlichting, *Chem. Rev.,* 2005, **105**, 2253-2278.
4 J. C. Price, E. W. Barr, B. Tirupati, J. M. Bollinger Jr. and C. Krebs, *Biochemistry*, 2003, **42**, 7497-7508.
5 S. Ye and F. Neese, *Proc. Natl. Acad. Sci. U. S. A.*, 2011, **108**, 1228-1233.
6 C. V. Sastri, J. Lee, K. Oh, Y. J. Lee, J. Lee, T. A. Jackson, K. Ray, H. Hirao, W. Shin, J. A. Halfen, J. Kim, L. Que Jr., S. Shaik and W. Nam, *Proc. Natl. Acad. Sci. U. S. A.*, 2007, **104**, 19181-19186.
7 J.-U. Rohde, J.-H. In, M. H. Lim, W. W. Brennessel, M. R. Bukowski, A. Stubna, E. Münk, W. Nam and L. Que Jr., *Science*, 2003, **299**, 1037-1039.
8 N. Y. Oh, Y. Suh, M. J. Park, M. S. Seo, J. Kim and W. Nam, *Angew. Chem., Int. Ed.*, 2005, **44**, 4235-4239.
9 J. Kaizer, E. J. Klinker, N. Y. Oh, J.-U. Rohde, W. J. Song, A. Stubna, J. Kim, E. Münck, W. Nam and L. Que Jr., *J. Am. Chem. Soc.* 2004, **126**, 472-477.
10 J. M. Mayer, *Acc. Chem. Res.*, 1998, **31**, 441-450.
11 D. Wang, M. Zhang, P. Buhlmann and L. Que Jr., *J. Am. Chem. Soc.*, 2010, **132**, 7638-7644.
12 J. Kaizer, E. J. Klinker, N. Y. Oh, J.-U Rohde, W. J. Song, A. Stubna, J. Kim, E. Münk, W. Nam and L. Que Jr., *J. Am. Chem. Soc.*, 2004, **126**, 472-473.
13 T. Chantarojsiri, Y. Sun, J. R. Long and C. J. Chang, *Inorg. Chem.* 2015, **54**, 5879-5887.
14 J. M. Smith and J. R. Long, *Inorg. Chem.*, 2010, **49**, 11223-11230.
15 Y. Shimoyama, T. Ishizuka, H. Kotani, Y. Shiota, K. Yoshizawa, K. Mieda, T. Ogura, T. Okajima, S. Nozawa, T. Kojima, *Angew. Chem., Int. Ed.*, 2016, **55**, 14041-14045.
16 Y. Shimoyama, T. Ishizuka, H. Kotani, T. Kojima, *ACS Catal.*, 2019, **9**, 671-678.
17 Y. Shimoyama and T. Kojima, *Inorg. Chem.*, 2019, **58**, 9517-9542.
18 In the asymmetric unit, two independent moieties of **1** were inluded. Thus, the bond length is the mean vaue of the two independent molecules of **1**.
19 Although BDE of the benzylic C-H bonds in EtPhS is higher than that in CumS, the TONs divided by the number (*n*) of the equivalent C-H bonds in the substrates were almost the same: 21 for EtPhS (*n* = 2) and 26 for CumS (*n* = 1).
20 M. Ghosh, K. K. Singh, C. Panda, A. Weits, M. P. Hendrich, T. J. Collins, B. B. Dhar and S. S. Gupta, *J. Am. Chem. Soc.*, 2014, **136**, 9524-9527.
21 To confirm that the oxygen atoms of $Na_2S_2O_8$ do not exchange with solvent water molecules, IR spectra of $Na_2S_2O_8$ were measured before and after the treatment with $H_2{}^{18}O$ and the spectra were almost the same without any shifts of the S=O and O-O stretching bands (Fig. S10).
22 I. Garcia-Bosch, A. Company, C. W. Cady, S. Styring, W. R. Browne, X. Ribas and M. Costas, *Angew. Chem., Int. Ed.*, 2011, **50**, 5648-5653.
23 E. A. Mader, E. R. Davidson and J. M. Mayer, *J. Am. Chem. Soc.*, 2007, **129**, 5153-5166.
24 Y.-R. Luo, *Handbook of bond dissociation energies in organic compounds,* 2003.
25 M. Finn, R. Friedline, N. K. Suleman, C. J. Wohl and J. M. Tanko, *J. Am. Chem. Soc.*, 2004, **126**, 7578-7584.
26 A high reduction potential of $SO_4^{\bullet-}$ has been reported to be +2.19 V *vs.* SCE in water. R. E. Huie, C. L. Clifton and P. Neta, *Int. J. Radiat. Appl.Instrum. C*, 1991, **38**, 477-481.

TOC